Plant Science

Stomatal and non-stomatal limitations in savanna trees and C_4 grasses grown at low, ambient and high atmospheric CO_2

Chandra Bellasio[a, 1–4*], Joe Quirk[a, 1], and David J. Beerling[1]

[1] *Department of Animal and Plant Sciences, University of Sheffield, Sheffield, S10 2TN, UK.*

[2] *Research School of Biology, Australian National University, Acton, ACT, 2601 Australia.*

[3] *University of the Balearic Islands 07122 Palma, Illes Balears, Spain.*

[4] *Trees and Timber institute, National Research Council of Italy, 50019 Sesto Fiorentino (Florence).*

[a] Contributed equally to this work *Correspondence: chandra.bellasio@anu.edu.au

Abstract

By the end of the century, atmospheric CO_2 concentration ($[CO_2]_a$) could reach 800 ppm, having risen from ~200 ppm ~24 Myr ago. Carbon dioxide enters plant leaves through stomata that limit CO_2 diffusion and assimilation, imposing stomatal limitation (L_S). Other factors limiting assimilation are collectively called non-stomatal limitations (L_{NS}). C_4 photosynthesis concentrates CO_2 around Rubisco, typically reducing L_S. C_4-dominated savanna grasslands expanded under low $[CO_2]_a$ and are metastable ecosystems where the response of trees and C_4 grasses to rising $[CO_2]_a$ will determine shifting vegetation patterns. How L_S and L_{NS} differ between savanna trees and C_4 grasses under different $[CO_2]_a$ will govern the responses of CO_2 fixation and plant cover to $[CO_2]_a$ – but quantitative comparisons are lacking. We measured assimilation, within soil wetting–drying cycles, of three C_3 trees and three C_4 grasses grown at 200, 400 or 800 ppm $[CO_2]_a$. Using assimilation–response curves, we resolved L_S and L_{NS} and show that rising $[CO_2]_a$ alleviated L_S, particularly for the C_3 trees, but L_{NS} was unaffected and remained substantially higher for the grasses across all $[CO_2]_a$ treatments. Because L_{NS} incurs higher metabolic costs and recovery compared with L_S, our findings indicate that C_4 grasses will be comparatively disadvantaged as $[CO_2]_a$ rises.

Keywords

Photosynthesis, elevated CO_2, global change, Poaceae, acacia, *Vachellia*, *Celtis*, *Combretum*, non-stomatal limitations, sub-ambient CO_2.

Short title

Photosynthetic limitations and acclimation of savanna plants at low-to-high $[CO_2]_a$

Introduction

All photosynthetic organisms use the same ancestral C_3 biochemical machinery in which CO_2 is fixed by ribulose 1,5-bisphosphate carboxylase/oxygenase (Rubisco) and the products are processed into sugars by dark reactions. In C_3 plants, CO_2 reaches Rubisco along a CO_2 diffusion gradient from higher atmospheric, to lower chloroplastic concentrations [1]. CO_2 diffuses into leaves through stomata – the same pathway as water vapour out – and plants regulate the rate of gas exchange by adjusting stomatal conductance (g_S) through changes in stomatal density, dimensions and aperture, which regulate evapotranspiration (E) [2]. Stomata therefore limit CO_2 diffusion into leaves and the [CO_2] in sub-stomatal cavities (C_i) [3], and the extent of this limitation is called stomatal limitation (L_S). Stomata respond, not exclusively, to temperature, atmospheric humidity and CO_2 concentration ($[CO_2]_a$), and the amount of water within and supplied to leaves from the soil [4]. Limitations to A caused by other leaf-level constraints are called non-stomatal limitation, L_{NS}, and include intercellular and intracellular CO_2 diffusion, light, metabolic and biochemical constraints (Rubisco capacity, adenosine triphosphate [ATP] availability, ribulose 1,5-bisphosphate [RuBP] synthesis, and leaf nitrogen), source–sink dynamics, and leaf ultrastructure [5, 6].

Rubisco can either carboxylate or oxygenate RuBP in competing photosynthetic and photrespiratory reactions. Photorespiration metabolises already fixed carbon, evolving CO_2 and offsetting net CO_2 uptake [7-9], and is largely determined by the ratio of O_2 : CO_2 concentration at the Rubisco catalytic sites [8, 10]. C_4 photosynthesis reduces photorespiration by decreasing O_2 : CO_2 with a CO_2-concentrating mechanism (CCM) [11]. The C_4 pathway evolved independently ~60 times in >18 families [12, 13], many of which appeared in the Neogene (beginning ~23 Myr ago) after a reduction in $[CO_2]_a$ from ~1000 ppm towards 180 ppm [14, 15]. Subsequently, savanna ecosystems expanded at the expense of closed forests under low $[CO_2]_a$ on all continents over the last 10–25 Myr [14] as monsoon-driven seasonal aridity increased [16, 17]; and C_4-dominated grasslands generally expanded from mixed C_3 and C_4 grasslands ~9 Myr ago [14, 18, 19]. Chronic disturbance from herbivory and fires, fuelled by productive and flammable C_4 grasses, supress tree recruitment and promote open habitats, meaning savanna vegetation patterns are closely linked to the productivity of C_4 grasslands [20-23]. Changes in disturbance drivers can induce rapid transition between open, C_4-dominated grasslands with scattered trees, and closed forest [24, 25], and savanna vegetation responses to disturbance are likely to be modified by changing $[CO_2]_a$.

Today, savannas experience $[CO_2]_a$ levels that are higher than in any point during their evolutionary history, but the effect of rising $[CO_2]_a$ on savanna vegetation patterns is difficult to predict, in part because potential differences in the relative roles of stomatal and non-stomatal limitations in the photosynthetic responses of C_3 and C_4 plants to $[CO_2]_a$ are not well understood [22, 26-29]. When stomatal factors limit photosynthesis during a drought, for example, A is

restored by increasing C_i through stomatal opening upon restoration of soil water availability; consequently, L_S does not impair or reduce metabolic function [6, 30, 31]. Conversely, metabolic constraints imposed by L_{NS} are generally not immediately relieved with increases in soil water and g_S, necessitating metabolic repair and prolonging recovery of A to pre-drought levels [32]. Under mild water limitation – that might be experienced daily or weekly in open, semiarid savannas – L_S is thought to predominate limitations to A in C_4 leaves, with L_{NS} becoming more important as leaf water status continues to decline [6, 33, 34]. However, compared with C_3, C_4 leaves are more susceptible to L_{NS} [32, 35] and the speed of leaf dehydration may govern the mode of limitation to A [35]. Although the severity of water limitation affects the relative influence of L_S and L_{NS}, few studies have assessed stomatal and metabolic contributions to C_3 and C_4 photosynthetic inhibition under moderate soil drying. Consequently, the extent and proportionality of stomatal and metabolic inhibition of A with moderate reductions in leaf water status are largely unknown for either C_3 or C_4 plants. Moreover, absolute declines in g_S with increasing growth $[CO_2]_a$ are generally larger for C_3 than C_4 leaves [10, 36]. If, however, C_4 plants suffer from increased L_{NS} relative to C_3 under moderate fluctuations in water availability this will impinge on their performance even under future rises in $[CO_2]_a$. Quantifying these processes will be important for predicting shifts in savanna vegetation patterns.

Here we aim to resolve how the relative contributions of L_S and L_{NS} respond to $[CO_2]_a$ and affect CO_2 fixation in C_3 forest and savanna trees and C_4 savanna grasses. We measured photosynthesis in three tree species (*Vachellia karroo*, *Celtis africana* and *Combretum apiculatum*) and three C_4 grass species (*Eragrostis curvula*, *Heteropogon contortus* and *Themeda triandra*) grown at either low (200 ppm), ambient (400 ppm) or elevated (800 ppm) $[CO_2]_a$. We grew the plants in replicated controlled-environment growth chambers and measured photosynthetic potential over typical wetting–drying cycles by watering plants to 80% of pot capacity and allowing soil moisture to decline over 2–3 days during which measurements were taken. We characterised photosynthetic potential with A–response measurements to parameterise empirical models for direct comparison between the trees and grasses, quantify L_S and L_{NS}, and assess differences in the $[CO_2]_a$-acclimation responses of the trees and grasses.

Materials and Methods

Plants and growth conditions

Seeds of *Vachellia karroo* (Hayne) (formerly *Acacia karroo*) were obtained from the Desert Legume Program, (Tucson, AZ, US), and both *Combretum apiculatum* (Sond.) and *Celtis africana* (N.L.Burm.) from Silverhill Seeds (Cape Town, ZA). *V. karroo* is a leguminous tree typical of open savannas, *Combretum* spp. are common in miombo closed savanna woodland, and *C. africana* is a forest tree. Germinated seeds were randomly distributed between six controlled-environment

growth chambers (Conviron BDR16, Conviron, Manitoba, CA) and grown for 18 months prior to measurements. C_4 grass seeds of *Eragrostis curvula* ([Schrad.] Nees) (accession number PI-155434), *Heteropogon contortus* ([L.] P.Beauv. ex Roem. & Schult.) (PI-228888) and *Themeda triandra* (Forssk.) (PI-208024) were obtained from the Germplasm Resources Information Network (GRIN, Agricultural Research Service, USDA, Washington D. C., US). These grasses span a range of adaptations to fire and drought and are broadly representative of open African savannas. Once established, a plant from each grass species was randomly selected, split into individuals at the rhizome, distributed between the growth chambers, and grown for 12 months prior to measurements. For clarity we refer to the plants by genus from here on.

Plants were grown in 2.5 dm^3 pots (n = 4–10) filled with three-parts commercial loam-free top soil (Boughton Ltd. Kettering, GB) plus one-part John Innes No.3 compost (John Innes Manufacturers Association, Reading, GB). Growth chambers (two per $[CO_2]_a$ treatment) were maintained at three $[CO_2]_a$ levels of 200, 400, or 800 ppm and otherwise constant conditions of 26 : 17 °C and 70 : 50 % relative humidity (day : night). A 12-hr photoperiod with a midday peak photosynthetic photon flux density (*PPFD*) of 800 μmol m^{-2} s^{-1} was imposed at canopy level. Light was provided from a 3:1 mix of 39-W white-fluorescent tubes (Master TL5, Philips, Eindhoven, NL) and 39-W red–blue fluorescent tubes (Grolux T5, Havells-Sylvania, Newhaven, GB), augmented with six 105-W halogen light bulbs (GLS, Havells-Sylvania). Plants were rotated weekly within, and monthly between, cabinets along with environmental settings to minimise block effects. From the outset, plants were watered to gravimetrically determined 80 % pot capacity three times per week after 24–32 photoperiod hours since last watering and all pots were provided with 150 ml of 3:1:2 N:P:K soluble nutrient mix (Miracle-Gro® All Purpose Plant Feed, Scotts Miracle-Gro, Marysville, OH, US) diluted to (5g nutrient mix l^{-1} water) every two or three weeks as part of the watering volume.

Leaf gas exchange and water potential

Instantaneous mid-afternoon leaf gas exchange was measured three times over six weeks on all plants using an infrared gas analyser, IRGA (LI6400XT, LI-COR Biosciences, Lincoln, NE, US) fitted with a 6 cm^2 cuvette and a red–blue LED light source (6400-02B, LI-COR Biosciences) under operational environmental conditions (denoted by subscript '$_{op}$') within the growth chambers after ~12 photoperiod hours since watering on young, fully expanded leaves. Two to four grasses blades were carefully aligned side by side and held together with insulation tape, avoiding any overlapping between blades, and clamped between the gaskets such that the area of the gas exchange cuvette was filled entirely. Where tree leaves did not fill the cuvette we made leaf area measurements using scaled, digital images of each leaf, taken while still attached to the plant using a bespoke leaf clamp and camera stand. Leaf area was calculated using ImageJ software (NIH, Bethesda, MA, US) and was used to correct gas exchange data at the time of measurement.

To minimise environmental perturbations and the time for leaf gas exchange to stabilise, the cuvette and integrated gas analyser was placed inside the growth chambers, which were opened briefly to switch plants between measurements, while air was supplied from within the closed chambers to the IRGA console outside using plastic tubing and CO_2 was supplied from cartridges (Liss–Group, Répcelak, HU). We set reference air [CO_2] (C_a, 200, 400 or 800 µmol mol^{-1}), block temperature (26°C) and light intensity (500 µmol m^{-2} s^{-1}) in the cuvette to correspond to those of the growth chambers at the time of measurement (mid-afternoon), set a flow rate of 235 µmol s^{-1} and took a 10-s average reading after readings had stabilised. Pilot studies indicated that this regime, particularly *PPFD* of the growth and measuring environment, ensured optimal growth for both trees and grasses and captured responses between fully lit and shaded leaves. During operational leaf gas exchange measurements, we sampled an adjacent, young, fully expanded leaf from each plant and immediately determined midday leaf water potential (Ψ_{leaf}) using a Scholander pressure chamber (PMS Instrument Company, Model 1000, Albany, OR, US). Simultaneous leaf sampling ensured we had an indicator of leaf water status at the time of leaf gas exchange measurement.

To derive photosynthetic model parameters (see A–*response curve analysis and photosynthetic parameters*), responses of net leaf *A* to C_i and *PPFD* (*A*–C_i and *A*–*PPFD* response curves) were measured after watering on a subsample of three to six randomly selected plants per species × $[CO_2]_a$ treatment using the same (trees) or similar (grasses) leaves to those used for operational gas exchange measurements. *A*–response curves were measured at the bench using the same IRGA as before, supplied with humidified ambient air adjusted to 60–70 % relative humidity and CO_2 from cartridges. Block temperature was 26 °C and flow rate was 235 µmol s^{-1} for both operational and *A*–response measurements and the leaf-to-boundary layer water mole fraction gradient within the cuvette (D_S) was < 20 mmol mol^{-1} during gas exchange measurements. This corresponds to an atmospheric vapour pressure deficit of < 2 kPa, which is unlikely to have induced significant stomatal limitation of assimilation . For *A*–*PPFD* curves, reference CO_2 was 200, 400 or 800 µmol mol^{-1} according to experimental growth $[CO_2]_a$ treatment, and for *A*–C_i curves *PPFD* was 1500 µmol m^{-2} s^{-1}. Leaves were acclimated for 30–60 min to reach full photosynthetic induction before automated *A*–response measurement routines were launched. The sample and reference IRGAs were matched before each measurement, mass flow leaks were sealed with water based putty, primary data were corrected for CO_2 diffusion, and C_i was recalculated after Bellasio *et al*. [37, 38].

A–response curve analysis and photosynthetic parameters

Comprehensive sets of fitted enzyme- and light-limited photosynthetic parameters (Tables 1 and 3) were derived from *A*–response curves within the framework of Bellasio, Beerling and Griffiths [37] and [38]. The dependence of gross assimilation (*GA*) on *PPFD* was modelled empirically as a non-

rectangular hyperbola parametrised using means from the species × $[CO_2]_a$ treatment level after Prioul and Chartier [39] as described in Bellasio, Beerling and Griffiths [37]:

$$GA = \frac{Y(CO_2)_{\mathrm{LL}}\ PPFD + GA_{\mathrm{SAT}} - \sqrt{(Y(CO_2)_{\mathrm{LL}}\ PPFD + GA_{\mathrm{SAT}})^2 - 4\ m\ Y(CO_2)_{\mathrm{LL}}\ PPFD\ GA_{\mathrm{SAT}}}}{2\ m}. \quad (1)$$

GA_{SAT} defines the horizontal asymptote and represents the light-saturated rate of *GA* under the $[CO_2]$ of the measurements. $Y(CO_2)_{\mathrm{LL}}$ describes the maximal quantum yield for CO_2 fixation, that is the conversion efficiency of *PPFD* into fixed CO_2 under the $[CO_2]$ of the measurements, and represents the inclined asymptote. m is an empirical factor ($0 \leq m \leq 1$) defining curvature. These parameters were estimated together with respiration in the light (R_{LIGHT}=*GA*-*A*) in a single step by fitting Eqn 1 to *A*–*PPFD* curves using the fitting tool of ref. [37], note that this method does not require fluorescence data and was described in the video tutorial 'additional features' [http://youtu.be/fEZkujIfesc].

The relationship between *A* and C_i was modelled empirically as a non-rectangular hyperbola, analogous to Eqn 1, parametrised using treatment means at the species × $[CO_2]_a$ treatment level, describing potential assimilation (A_{pot}) for a given C_i under optimal conditions after Bellasio, Beerling and Griffiths [37] as:

$$A_{\mathrm{pot}} = \frac{CE(C_i - \Gamma) + A_{\mathrm{SAT}} - \sqrt{(CE[C_i - \Gamma] + A_{\mathrm{SAT}})^2 - (4\omega A_{\mathrm{SAT}} CE[C_i - \Gamma])}}{2\omega}, \quad (2)$$

where A_{SAT} represents the CO_2-saturated rate of *A* under the *PPFD* of the measurements and defines the horizontal asymptote. *CE* is maximal carboxylating efficiency for CO_2 fixation (*CE*), and defines the inclined asymptote. ω is an empirical factor ($0 \leq \omega \leq 1$) defining curvature.

Stomatal and non-stomatal limitation to A

The limitation to *A* imposed by stomata (stomatal limitation, L_S) was determined analogously to Farquhar and Sharkey [40] using Eqn 2 for each species × $[CO_2]_a$ treatment (Table 1) and was calculated after [37, 38] as:

$$L_S = \frac{A_{\mathrm{potCa}} - A_{\mathrm{pot}Ciop}}{A_{\mathrm{potCa}}}, \quad (3)$$

and non-stomatal limitation (L_{NS}), defining limitations to *A* not related to physical stomatal density, dimensions or aperture, was calculated after Bjorkman, Downton and Mooney [41] as:

$$L_{\mathrm{NS}} = \frac{A_{\mathrm{potCiop}} - A_{\mathrm{op}}}{A_{\mathrm{potCa}}}, \quad (4)$$

where A_{potCa} is the *A* that would occur, as predicted by the *A*–C_i curve, if there was no epidermal impediment to CO_2 diffusion into the leaf such that C_i was equal to ambient $[CO_2]$ at the leaf surface (C_a) (Figure 1). A_{potCiop} is the *A* that would occur, as predicted by the *A*–C_i curve, when C_i

equals C_{iop} (C_i under operational growth conditions, Figure 1) [42]. A_{potCa} and $A_{potCiop}$ were calculated from Eqn 2 by solving for C_i=C_a and C_i=C_{iop}.

Statistical analysis

The effects of species (nested within photosynthetic type), $[CO_2]_a$, and their interaction on operational gas exchange measurements, D_S in the leaf chamber, L_S, L_{NS}, Ψ_{leaf} and fitted photosynthetic parameters (Table 1) were tested with two-way ANOVA using a general linear model (GLM) framework following appropriate transformation to satisfy assumptions of homogeneity of variance (details of data transformation are listed in Tables 2 and 3). Specific differences between means of L_S and L_{NS} were tested with *post-hoc* Tukey pairwise comparisons. The level of biological replication was n = 4–10 (as indicated) for operational gas exchange data, L_S, L_{NS} and Ψ_{leaf} (in which biological replicates are the mean of triplicate technical replicates) and n = 3–6 (as indicated) for photosynthetic parameters derived from A–response curves. All ANOVA models were fitted and analysed in Minitab v.17 (Minitab Inc., State College, PA, US) with a significance threshold of 95 %.

Results

Gas exchange under operational conditions

Measurements of gas exchange under operational conditions ('$_{op}$') (Figure 2) were carried out in the middle of the drying cycle after 24–28 hours since watering to 80% pot capacity. Increased growth $[CO_2]_a$ stimulated leaf assimilation (A_{op}) in both the trees and the C_4 grasses except *Eragrostis*, but there were notable species differences within photosynthetic type (Figure 2A; Table 2). The reduction in growth $[CO_2]_a$ from 400 ppm to 200 ppm led to a decline in A_{op} of 45% on average across the three tree species (*Vachellia* −38%, *Celtis* −60% and *Combretum* −37%). With the rise in growth $[CO_2]_a$ from 400 ppm to 800 ppm, A_{op} for the trees increased by 77% on average (*Vachellia* +60%, *Celtis* +63% and *Combretum* +109%). The CO_2-fertilisation effect on A_{op} for the trees was stronger with the increase in growth $[CO_2]_a$ from 200 ppm to 400 ppm than from 400 ppm to 800 ppm (Figure 2A; Table 2).

For the grasses, A_{op} declined by an average of −30% with the decline in growth $[CO_2]_a$ from 400 ppm to 200 ppm, but variation between species was high, with an increase in A_{op} of 8% for *Eragrostis* being offset by decreases of −48% and −49% for *Heteropogon* and *Themeda*, respectively (Figure 2A). Differences in the responses of the grass species to growth $[CO_2]_a$ were maintained with the increase from 400 ppm to 800 ppm. *Eragrostis* A_{op} was least responsive to the increase in $[CO_2]_a$ (+1%), whereas A_{op} for *Heteropogon* (+28%) and *Themeda* (+106%) was much more responsive. Assimilation in *Eragrostis* leaves was offset by relatively high rates of daylight respiration (R_{LIGHT}), particularly at higher growth $[CO_2]_a$ (Table 1).

For all species except *Celtis*, stomatal conductance (g_S) and leaf-level evapotranspiration (E_{op}) increased as growth $[CO_2]_a$ declined from 400 ppm to 200 ppm (Figure 2B–C; Table 2; +25% g_{Sop} and +28% E_{op} on average for the trees and +61% g_{Sop} and +78% E_{op} on average for the C_4 grasses). In contrast, g_{Sop} and E_{op} were less responsive to the increase in growth $[CO_2]_a$ from 400 ppm to 800 ppm (Figure 2B–C; Table 2; −5% g_{Sop} and −16% E_{op} on average for the trees and −18% g_{Sop} and −25% E_{op} on average for the C_4 grasses).

The mean (Figure 2D) and range (Figure 3) of C_{iop} increased progressively with growth $[CO_2]_a$ for both the trees and the grasses (Table 2). The increase in C_{iop} with growth $[CO_2]_a$ was generally linear for all species except *Heteropogon*, which showed no apparent change in C_i with the increase in $[CO_2]_a$ from 200 ppm to 400 ppm (Figure 2D). At 200 ppm $[CO_2]_a$, C_i clustered around low values but the range of values became increasingly spread at higher growth $[CO_2]_a$ in a manner that was independent of photosynthetic type.

With the exception of *Eragrostis*, the leaf-to-boundary layer water vapour mole fraction (D_S) within the leaf chamber during gas exchange measurements generally declined with increasing growth $[CO_2]_a$ (Figure 2E; Table 2). Declines were steeper between 200 ppm and 400 ppm than 400 ppm and 800 ppm, reflecting the trend in g_{Sop} and E_{op}, but D_S for *Eragrostis* was apparently independent of g_S (Figure 2B–C). Day time leaf water potential (Ψ_{leaf}) generally increased non-linearly with growth $[CO_2]_a$, with steeper responses for all species except *Vachellia* and C_4 *Heteropogon* between 200 ppm and 400 ppm $[CO_2]_a$ than between 400 ppm and 800 ppm (Figure 2F; Table 2). Under each growth $[CO_2]_a$, Ψ_{leaf} varied more between tree species than C_4 grasses. The savanna tree, *Vachellia* operated at the lowest Ψ_{leaf} (most negative) across all $[CO_2]_a$ levels, reflecting its relatively high rates of g_S, E_{op} and A_{op} (Figure 2A–C).

A–*response curves*

The *A*–response curves used to determine A_{pot} were measured at 80% of pot capacity. The light curves revealed that at high *PPFD*, *A* increased progressively with increasing growth $[CO_2]_a$ for all the tree species, but the trend was most pronounced for *Vachellia* (Figure 4). Amongst the C_4 grasses, *Heteropogon* and *Themeda* showed a similar trend as the trees in which *A* at high *PPFD* increased with growth $[CO_2]_a$, but *Eragrostis* displayed high *A* across all growth $[CO_2]_a$ levels. At 200 ppm $[CO_2]_a$ under high *PPFD*, *Eragrostis* had at least 4-fold higher *A* compared with all other species, but C_4 *Heteropogon* and *Themeda* attained similar rates to *Vachellia* – almost double those of *Celtis* and *Combretum* (Figure 4; GA_{SAT} in Table 1). The *A*–C_i response curves were consistently steeper for the grasses than trees, especially those grown at 200 ppm $[CO_2]_a$, but CO_2-saturated rates of *A* showed greater differences between species than between C_3 trees and C_4 grasses across all $[CO_2]_a$ (Figure 5).

Potential rates of assimilation determined from photosynthetic parameters

The *A–PPFD* and A–C_i response curves were used to derive a suite of photosynthetic parameters (Table 1). The CO_2-saturated rate of assimilation (A_{SAT}) was not affected by growth $[CO_2]_a$, but was consistently ~39% higher for the trees than grasses across growth $[CO_2]_a$ (Table 1 and 2). The initial slope of the A–C_i curves, called carboxylation efficiency (*CE*), was generally 2–3-fold higher for the C_4 grasses than trees, and declined with increasing growth $[CO_2]_a$ across all species except *Celtis* (Tables 1 and 3). *CE* decreased by 34% in *Eragrostis*, 79% in *Heteropogon* and 26% in *Themeda*, compared with a marginal decrease of 18% in *Vachellia* and 56% decrease in *Combretum*, while *Celtis* showed no downregulation of *CE* (Table 1). Accordingly, the CO_2 compensation point (Γ, the C_i at which A is zero) was ~94% higher for trees across $[CO_2]_a$, and overall increased with growth $[CO_2]_a$ (Table 1 and 2).

The light-saturated rate of gross assimilation (GA_{SAT}) increased with growth $[CO_2]_a$ for all species except *Eragrostis*, which maintained consistently high GA_{SAT} across $[CO_2]_a$; but GA_{SAT} was generally less responsive to growth $[CO_2]_a$ for the grasses than trees. For the C_4 grasses, GA_{SAT} was 60% higher compared with the trees at 200 ppm $[CO_2]_a$, 19% higher at 400 ppm, but was 25% lower than the trees at 800 ppm $[CO_2]_a$ (Table 1). Quantum yield of CO_2 fixation [$Y(CO_2)_{LL}$ – a measure of light-use efficiency, for comparison with other studies note that here it is expressed on incident light basis] increased sharply with increases in growth $[CO_2]_a$ for the trees, but showed no variation for C_4 *Eragrostis* and *Heteropogon*, and a slight increase for *Themeda*. Overall, $Y(CO_2)_{LL}$ was 23% lower for trees than grasses at 200 ppm, but this was reversed at 800 ppm $[CO_2]_a$ where $Y(CO_2)_{LL}$ was 36% higher for trees. The light compensation point (*LCP – PPFD* at which A is zero) was generally unaffected by growth $[CO_2]_a$ for C_4 *Eragrostis* and *Heteropogon*. Daylight mitochondrial respiration (R_{LIGHT}) was 40% higher for grasses than trees at 200 ppm $[CO_2]_a$, 20% higher at 400 ppm (Table 1 and 2), driven by substantial increases in R_{LIGHT} for trees grown at higher $[CO_2]_a$.

Operational and potential rates of assimilation

The values of A_{op} and C_{iop} obtained from within-cabinet measurements (shown as points in Figure 3) can be compared with empirically modelled A–C_i curves parameterised with species × $[CO_2]_a$ treatment means (lines in Figure 3). The A–C_i curves were measured on young, fully expanded leaves of well-watered plants, under controlled laboratory conditions, meaning many of the limitations present in the growth cabinets were minimised, and we refer to these conditions as those allowing a 'potential' rate of leaf-level assimilation (A_{pot}). The distance between the datapoints and the modelled curves, therefore, indicates the degree to which leaf-level A_{op} was limited by conditions imposed by the growth environment. Comparison of the datapoints with the curves in Figure 3 indicates that plants grown at 200 ppm $[CO_2]_a$ generally assimilated CO_2 closer to their

potential rates compared with plants grown at higher $[CO_2]_a$, and that the C_3 trees tended to operate closer to their potential compared with the grasses. C_4 grasses grown at 800 ppm $[CO_2]_a$ operated at rates that were on average 38% lower than potential rates. A_{op} for some plants was higher than the modelled A–C_i curves (parameterised with mean values from the sub-sample of plants randomly selected for A–response measurements), indicating those individuals were operating closer to potential rates within the growth chambers. The distance between potential and actual assimilation was quantified and resolved in stomatal and non-stomatal limitations to assimilation.

Quantifying non-stomatal limitations to assimilation

We calculated stomatal (L_S) and non-stomatal limitations (L_{NS}) to assimilation through empirical modelling (Eqn 1), using parameters derived at the species × $[CO_2]_a$ level (Table 1). L_S are diffusional limitations imposed by stomatal closure and are mediated by lower values of C_i. Using the A–C_i curve, L_S is the relative difference between the value of A when C_i is equal to C_a and the value of A when C_i is equal to C_{iop} (Eqn 3; Figure 1). L_{NS} include sink limitations, incomplete photosynthetic induction, light limitation, limitation to triose phosphate use (which is unlikely under the growth conditions here), but not down-regulation of photosynthetic potential (V_{CMAX}, V_{PMAX}, J_{SAT} – see *Discussion*). L_{NS} can be visualised for each datapoint as the relative difference between the value of within-cabinet A_{op} and the value of A when C_i is equal to C_{iop} along the A–C_i curve (Eqn 4; Figure 1).

The primary limitation to photosynthesis for the C_4 grasses was L_{NS} across growth $[CO_2]_a$ levels, whereas the trees experienced proportionally higher L_S, particularly when grown at 200 ppm $[CO_2]_a$ (Figure 6 dotted lines and grey shading; Table 3). For the C_4 grasses, L_{NS} was 56% – 100% higher on average, whereas L_S was 60% – 76% lower on average compared with the trees across $[CO_2]_a$ treatments, with the largest differences observed at 200 ppm $[CO_2]_a$ (Figure 6; Table 3), in line with previous reports [30-32, 34, 35]. L_S declined significantly as growth $[CO_2]_a$ increased for both the trees and grasses, whereas L_{NS} responded less to $[CO_2]_a$; although for the grasses, L_{NS} declined marginally with increases in growth $[CO_2]_a$ (Figure 6; Table 3). At species level, for *Eragrostis* grown at 200 ppm $[CO_2]_a$, L_S was 92% higher compared with plants grown at 800 ppm $[CO_2]_a$ (0.22 vs 0.018), but this sensitivity to $[CO_2]_a$ was not significant for C_4 *Themeda* or *Heteropogon*.

For all three C_4 grasses, higher L_{NS} was generally linked with lower L_S, and this pattern was apparently independent of growth $[CO_2]_a$ for *Heteropogon* and *Themeda* (Figure 6). For *Eragrostis*, however, the relationship was driven more by effects of growth $[CO_2]_a$, whereby L_S was highest and L_{NS} was lowest for plants grown at 200 ppm $[CO_2]_a$ (Figure 6a and d). This indicates that for *Eragrostis*, metabolic factors became increasingly limiting as growth $[CO_2]_a$ increased. This pattern was also observed for *Celtis* trees, whereas for all the remaining tree and grass species, L_{NS} was lowest at 800 ppm $[CO_2]_a$ (Figure 6). Moreover, L_S for *Eragrostis* was remarkably high at 200 ppm $[CO_2]_a$ compared with the other C_4 grasses, and was similar to that of C_3 *Vachellia* (Figure 6a).

Discussion

Controlled-environment and field studies have generally shown that elevated $[CO_2]_a$ stimulates assimilation and growth of C_3 plants [43-45]. Studies have also found that C_4 plant growth can respond positively to elevated $[CO_2]_a$ under well-watered conditions [46-51]. The growth stimulation of C_4 plants in response to a doubling of ambient $[CO_2]_a$ (from 350–400 to 700–800 ppm) is, on average, about 22–33%, compared with 40–44% for C_3 plants [43, 44, 51, 52]. In C_3 plants, stimulated growth is attributed primarily to increases in leaf assimilation potential (A_{pot}). Although this mechanism has also been linked with stimulated growth of C_4 plants [47, 49-51, 53, 54], a number of studies have found a growth response in C_4 plants in the absence of enhanced leaf *A* [46, 55] or have found enhancement of leaf *A* in the absence of increased growth [49, 50].

In C_3 plants, acclimation to elevated $[CO_2]_a$ can induce down-regulation of the potential for carboxylation (Rubisco and other C_3 cycle enzymes), and is often accompanied by reduction in foliar nitrogen content and accumulation of carbohydrate reserves [56]. In C_4 plants, acclimation may involve down-regulation of PEPC activity [51, 54, 57], but this is not commonly observed. In our study we derived the carboxylating efficiency (*CE*), which is empirically based and allows comparison of both C_3 and C_4 enzymatic capacity without requiring assumptions of the underpinning biochemistry (for details see [37, 38]). Unexpectedly, and in contrast with previous reports [for review, Ghannoum, Caemmerer, Ziska and Conroy [58]], the pattern of down-regulation presented here was more pronounced in the C_4 grasses than the C_3 trees. The maximal rates of *A* observed for some of the species, notably *Heteropogon* and *Themeda*, were lower than expected (e.g. [32, 59, 60]). This may be partly due to differences between the environmental conditions in the growth chambers and those experienced by C_4 grasses in the field – but *Eragrostis* attained reasonably high rates of *A* under the same conditions – and partly by the absence of disturbance in our experiment. Observations indicate that *Themeda* all but disappears if disturbance is prevented, but dominates where disturbance is frequent [61, 62]. Burning, in particular, is an important factor in *Themeda* and *Heteropogon* growth and ecosystem dominance, and may stimulate higher productivity and photosynthetic rates. Interestingly, *Themeda* displayed traits that are not usual for a C_4 grass and this is supported by previous studies where *Themeda* was found to switch to an unexpected C_3-like behaviour when nitrogen supply was changed from nitrate to ammonium [63].

To allow higher rates of A_{op} at high $[CO_2]_a$, despite enzymatic down-regulation of carboxylating capacity, the biochemical machinery must be exploited more efficiently. In part, because it is the reaction substrate, high $[CO_2]_a$ allows Rubisco and PEPC to operate closer to CO_2 saturation, and, consequently, at a higher velocity. Indeed, here the composition of the photosynthetic machinery was shifted away from carboxylating capacity towards greater electron transport capacity. This was indicated by an increase in the empirical parameter, GA_{SAT}, which was consistently up-regulated to

a varying degree in all plants at higher $[CO_2]_a$, with trees showing stronger acclimation to growth $[CO_2]_a$ than the grasses (Table 1). A larger increase in electron transport capacity for the trees with increases in growth $[CO_2]_a$ was substantiated by increases in $Y(CO_2)_{LL}$ at higher growth $[CO_2]_a$, which were not observed for the grasses (Table 1).

Over the 2–3–day watering–drying cycle, despite a relatively moderate reduction in soil water, L_{NS} imposed a clear effect on C_4 CO_2 fixation, causing sufficient metabolic inhibition in the C_4 grasses to reduce A by ~40% compared with 20–30% for the trees, highlighting the sensitivity of C_4 photosynthesis to soil drying and reductions in leaf water status [64-66] (Figure 6). Non-stomatal limitation normally includes source-sink feedbacks, reduced substrate supply to carboxylases, limitations imposed by the diffusion of metabolites between M and BS cells, light limitation, CO_2 leakiness [67], and downregulation of photosynthetic potential. Here, the latter does not factor in the estimation of L_{NS} because A–C_i curves were purposely measured on the same or similar leaves to those on which A_{op} was measured. Our findings indicate that C_4 grasses could experience metabolic impairment of their photosynthetic machinery even with mild reductions in soil water availability that may be experienced over seasonal or even shorter timescales.

Transient decreases in leaf water status could form a central driver of L_{NS}, which may arise as a result of either soil or atmospheric water deficit. Under conditions of high midday radiation and temperature, leaves may experience substantial evaporative demands that induce transient decreases in leaf water status with adverse effects on A. However, we recognise that it is not straightforward to extrapolate from operating performance in pot experiments under intermediate *PPFD* to impacts of high radiation in a natural field setting where roots may extend to deeper water resources. Nevertheless, the C_4 photosynthetic pathway is more demanding both anatomically and biochemically than the C_3 pathway because it places metabolic demand on both the M and the BS, and requires continuous rapid exchange of metabolites between the two [68-70]. When leaf water status falls below a threshold, C_4 photosynthesis becomes quickly inhibited – a phenomenon that is captured experimentally by increasing L_{NS}. Comparative studies of closely related C_3 and C_4 grasses suggest that C_4 species experience greater L_{NS} during drought compared with C_3 species, which experience proportionally higher L_S [32, 66]. Ripley, Frole and Gilbert [32] found that L_{NS} accounted for 50% of the decline in A with declining soil moisture for C_4 grass species, compared with 25% for closely related C_3 species, and the predominance of L_{NS} over L_S prolonged the recovery of C_4 A following subsequent increases in soil moisture. This indicates that photosynthetic rates recover more quickly when inhibited by stomatal compared with metabolic factors.

The reduction in A associated with moderate drying in our study was not sufficient to curtail the photosynthetic advantage of the C_4 grasses over C_3 trees under operational conditions at low $[CO_2]_a$, particularly for *Eragrostis*. But the C_4 photosynthetic advantage over C_3 trees diminished at higher growth $[CO_2]_a$. This allowed the trees and *Celtis*, in particular to attain high rates of A_{op} that were generally higher than for the C_4 grasses at 800 ppm $[CO_2]_a$ (Figure 3). Under more severe soil

411 drying or cooler conditions, when C_4 grasses may be comparatively more susceptible than C_3
412 grasses [64], these effects could become more acute. There is evidence that C_4 grasses experience
413 L_{NS} under mild drought [33], and that the speed of leaf dehydration governs the mode of limitation
414 to *A*, whereby slower dehydration induces L_S and rapid dehydration is more likely to induce
415 metabolic inhibition [35]. Combined with Saccardy *et al*. [35], our findings indicate that chronic
416 L_{NS}, experienced during moderate drying, and potentially compounded during more severe drought
417 or winter frost, could impair C_4 metabolic function and impart long-term metabolic damage, thereby
418 offsetting the assimilatory advantage of C_4 grasses under optimal conditions. This represents an
419 overlooked factor in competitive interactions between trees and C_4 grasses and possibly between C_3
420 and C_4 grasses under changing $[CO_2]_a$, necessitating further studies into the hydraulic responses of
421 C_3 and C_4 plants to soil drying.

422 As our findings indicate, rising $[CO_2]_a$ over coming decades is more likely to alleviate L_S of C_3
423 leaves than C_4, whilst L_{NS} of both C_3 and C_4 leaves is likely to remain unaffected (Figure 6; Table
424 3). Savanna ecosystems are likely to be particularly sensitive to differential effects of rising $[CO_2]_a$
425 on L_S and L_{NS} for C_3 trees and C_4 grasses, which will affect CO_2 fixation and modify tree–grass
426 interactions and vegetation responses to changing $[CO_2]_a$. Combined with comparatively low L_{NS}
427 for the forest and woodland trees *Celtis* and *Combretum*, this indicates that C_3 trees will become
428 more competitive under rising $[CO_2]_a$ and may expand into open habitats, as supported by
429 theoretical analyses [71]. In a savanna context, greater competitiveness of forest and woodland
430 species under rising $[CO_2]_a$ could be critical, because, if the advantage in leaf-level CO_2 fixation
431 promotes growth and canopy expansion, C_4 grasses may become overshadowed leading to lower
432 grassy abundance and increasing woody encroachment.

433 **Conclusion**

434 Under a physiological watering–drying cycle, the assimilation of C_4 grasses was disproportionately
435 limited by metabolic factors that were not alleviated by increasing $[CO_2]_a$ of the growth
436 environment. In fact, for the C_4 grass with the highest rates of assimilation (*Eragrostis*), non-
437 stomatal limitations to assimilation increased at higher growth $[CO_2]_a$. A fraction of the non-
438 stomatal limitation in the C_4 grasses was likely caused by transient decreases in leaf water status
439 and linked by transpiration to stomatal limitation, although the mechanistic underpinnings remain
440 unresolved. In contrast, the inhibition of assimilation in C_3 forest trees due to stomatal factors
441 decreased substantially with increasing $[CO_2]_a$ and this was accompanied by substantial increases in
442 photosynthetic rates. Our findings indicate that with rising $[CO_2]_a$, limitations to photosynthesis
443 will be alleviated more for C_3 trees and grasses than C_4 grasses, which will reduce the
444 competitiveness of C_4 grasses to impinge on savanna vegetation patterns. Leaf-level processes
445 driving L_S and L_{NS} and their responses to $[CO_2]_a$ are not currently incorporated in mechanistic
446 predictions of savanna vegetation change under future climate scenarios [72]. We suggest that leaf

level inhibition of assimilation should be more widely considered in predictions of vegetation responses to environmental change [73]. Resolving the physiological underpinnings of L_{NS} and their relative contribution to photosynthetic inhibition is a pressing need.

Acknowledgments

We acknowledge funding through an ERC advanced grant (CDREG, 322998) awarded to DJB. CB acknowledges funding through a H2020 MSCA individual fellowship (DILIPHO, ID: 702755).

The authors have no conflict of interest.

Author contributions

CB, JQ and DJB designed the research. CB and JQ performed the measurements. CB and JQ analysed the data. JQ and CB wrote the paper with contributions from DJB.

References

[1] T. Tosens, Ü. Niinemets, V. Vislap, H. Eichelmann, P. Castro Díez, Developmental changes in mesophyll diffusion conductance and photosynthetic capacity under different light and water availabilities in *Populus tremula*: how structure constrains function, Plant, Cell & Environment, 35 (2012) 839-856.
[2] P.J. Franks, G.D. Farquhar, The mechanical diversity of stomata and its significance in gas-exchange control, Plant Physiol, 143 (2007) 78-87.
[3] J.R. Evans, S. von Caemmerer, Carbon dioxide diffusion inside leaves, Plant Physiol, 110 (1996) 339-346.
[4] P.G. Jarvis, The interpretation of the variations in leaf water potential and stomatal conductance found in canopies in the field, Philosophical Transactions of the Royal Society of London. B, Biological Sciences, 273 (1976) 593-610.
[5] D.W. Lawlor, Limitation to photosynthesis in water‐stressed leaves: stomata vs. metabolism and the role of ATP, Ann Bot-London, 89 (2002) 871-885.
[6] D.W. Lawlor, G. Cornic, Photosynthetic carbon assimilation and associated metabolism in relation to water deficits in higher plants, Plant, Cell & Environment, 25 (2002) 275-294.
[7] J. Ehleringer, O. Björkman, Quantum yields for CO_2 uptake in C_3 and C_4 plants: Dependence on temperature, CO_2, and O_2 concentration, Plant Physiology, 59 (1977) 86-90.
[8] J.R. Ehleringer, T.E. Cerling, Atmospheric CO_2 and the ratio of intercellular to ambient CO_2 concentrations in plants, Tree Physiology, 15 (1995) 105-111.
[9] F.A. Busch, T.L. Sage, A.B. Cousins, R.F. Sage, C3 plants enhance rates of photosynthesis by reassimilating photorespired and respired CO2, Plant, Cell & Environment, 36 (2013) 200-212.
[10] R.W. Pearcy, J. Ehleringer, Comparative ecophysiology of C3 and C4 plants, Plant, Cell & Environment, 7 (1984) 1-13.
[11] R.F. Sage, R.K. Monson, C_4 plant biology, Academic Press, San Diego, Calif. ; London, 1999.
[12] S.C. Morris, Evolutionary convergence, Current Biology, 16 (2006) R826-R827.
[13] R.F. Sage, A portrait of the C_4 photosynthetic family on the 50th anniversary of its discovery: species number, evolutionary lineages, and Hall of Fame, J. Exp. Bot., 68 (2017) e11-e28.
[14] E.J. Edwards, C.P. Osborne, C.A.E. Strömberg, S.A. Smith, C.G. Consortium, The origins of C_4 grasslands: Integrating evolutionary and ecosystem science, Science, 328 (2010) 587-591.
[15] P.A. Christin, C.P. Osborne, The evolutionary ecology of C_4 plants, New Phytol., 204 (2014) 765-781.
[16] J. Zachos, M. Pagani, L. Sloan, E. Thomas, K. Billups, Trends, rhythms, and aberrations in global climate 65 Ma to present, Science, 292 (2001) 686-693.
[17] A. Zhisheng, J.E. Kutzbach, W.L. Prell, S.C. Porter, Evolution of Asian monsoons and phased uplift of the Himalaya-Tibetan plateau since Late Miocene times, Nature, 411 (2001) 62-66.
[18] C.A.E. Strömberg, Evolution of grasses and grassland ecosystems, Annu. Rev. Earth Planet. Sci., 39 (2011) 517-544.
[19] C.P. Osborne, D.J. Beerling, Nature's green revolution: the remarkable evolutionary rise of C_4 plants, Philos. Trans. R. Soc. B-Biol. Sci., 361 (2006) 173-194.
[20] T. Charles-Dominique, T.J. Davies, G.P. Hempson, B.S. Bezeng, B.H. Daru, R.M. Kabongo, O. Maurin, A.M. Muasya, M. van der Bank, W.J. Bond, Spiny plants, mammal browsers, and the origin of African savannas, Proc. Natl. Acad. Sci. U.S.A., (2016).
[21] W.J. Bond, What limits trees in C_4 grasslands and savannas?, Annu. Rev. Ecol. Syst., 39 (2008) 641-659.
[22] W.J. Bond, G.F. Midgley, Carbon dioxide and the uneasy interactions of trees and savannah grasses, Philos. Trans. R. Soc. B-Biol. Sci., 367 (2012) 601-612.
[23] S. Hoetzel, L. Dupont, E. Schefusz, F. Rommerskirchen, G. Wefer, The role of fire in Miocene to Pliocene C_4 grassland and ecosystem evolution, Nature Geosci., 6 (2013) 1027-1030.
[24] M. Hirota, M. Holmgren, E.H. Van Nes, M. Scheffer, Global resilience of tropical forest and savanna to critical transitions, Science, 334 (2011) 232-235.
[25] A.C. Staver, S. Archibald, S.A. Levin, The global extent and determinants of savanna and forest as alternative biome states, Science, 334 (2011) 230-232.
[26] G.F. Midgley, W.J. Bond, Future of African terrestrial biodiversity and ecosystems under anthropogenic climate change, Nature Clim. Change, 5 (2015) 823-829.
[27] R.J. Scholes, S.R. Archer, Tree-grass interactions in savannas, Annual Review of Ecology and Systematics, 28 (1997) 517-544.
[28] A.C. Staver, Prediction and scale in savanna ecosystems, New Phytol., (2017) n/a-n/a.
[29] A.C. Staver, J. Botha, L. Hedin, Soils and fire jointly determine vegetation structure in an African savanna, New Phytol., 216 (2017) 1151-1160.
[30] O. Ghannoum, C_4 photosynthesis and water stress, Ann Bot-London, 103 (2009) 635-644.
[31] B.S. Ripley, M.E. Gilbert, D.G. Ibrahim, C.P. Osborne, Drought constraints on C4 photosynthesis: stomatal and metabolic limitations in C3 and C4 subspecies of Alloteropsis semialata, Journal of Experimental Botany, 58 (2007) 1351-1363.
[32] B. Ripley, K. Frole, M. Gilbert, Differences in drought sensitivities and photosynthetic limitations between co-occurring C_3 and C_4 (NADP-ME) Panicoid grasses, Annals of Botany, 105 (2010) 493-503.
[33] O. Ghannoum, J.P. Conroy, S.P. Driscoll, M.J. Paul, C.H. Foyer, D.W. Lawlor, Nonstomatal limitations are responsible for drought-induced photosynthetic inhibition in four C_4 grasses, New Phytologist, 159 (2003) 599-608.
[34] A. Lal, G. Edwards, Analysis of inhibition of photosynthesis under water stress in the C_4 species *Amaranthus cruentus* and *Zea mays*: electron transport, CO_2 fixation and carboxylation capacity, Functional Plant Biology, 23 (1996) 403-412.
[35] K. Saccardy, G. Cornic, J. Brulfert, A. Reyss, Effect of drought stress on net CO_2 uptake by *Zea* leaves, Planta, 199 (1996) 589-595.
[36] C.P. Osborne, L. Sack, Evolution of C_4 plants: a new hypothesis for an interaction of CO_2 and water relations mediated by plant hydraulics, Philos. Trans. R. Soc. B-Biol. Sci., 367 (2012) 583-600.
[37] C. Bellasio, D.J. Beerling, H. Griffiths, An Excel tool for deriving key photosynthetic parameters from combined gas exchange and chlorophyll fluorescence: theory and practice, Plant Cell Environ, 39 (2016) 1180–1197.
[38] C. Bellasio, D.J. Beerling, H. Griffiths, Deriving C_4 photosynthetic parameters from combined gas exchange and chlorophyll fluorescence using an Excel tool: theory and practice, Plant, Cell & Environment, 39 (2016) 1164-1179.
[39] J.L. Prioul, P. Chartier, Partitioning of Transfer and Carboxylation Components of Intracellular Resistance to Photosynthetic CO2 Fixation: A Critical Analysis of the Methods Used, Ann Bot-London, 41 (1977) 789-800.
[40] G.D. Farquhar, T.D. Sharkey, Stomatal conductance and photosynthesis, Annual Review of Plant Physiology, 33 (1982) 317-345.
[41] O. Bjorkman, W. Downton, H. Mooney, Response and adaptation to water stress in *Nerium oleander*, Annual Report-Carnegie Institution of Washington, Dept of Plant Biology (USA), (1979).
[42] H.G. Jones, Partitioning stomatal and non‐stomatal limitations to photosynthesis, Plant, Cell & Environment, 8 (1985) 95-104.
[43] H. Poorter, Interspecific variation in the growth response of plants to an elevated ambient CO_2 concentration, in: J. Rozema, H. Lambers, S.C. Van de Geijn, M.L. Cambridge (Eds.) CO_2 and Biosphere, Springer Netherlands, Dordrecht, 1993, pp. 77-98.
[44] H. Poorter, M.-L. Navas, Plant growth and competition at elevated CO_2: on winners, losers and functional groups, New Phytol., 157 (2003) 175-198.
[45] K.E. Idso, S.B. Idso, Plant responses to atmospheric CO_2 enrichment in the face of environmental constraints: a review of the past 10 years' research, Agric. Forest Meteorology, 69 (1994) 153-203.
[46] O. Ghannoum, S.v. Caemmerer, E.W.R. Barlow, J.P. Conroy, The effect of CO_2 enrichment and irradiance on the growth, morphology and gas exchange of a C_3 (*Panicum laxum*) and a C_4 (*Panicum antidotale*) grass, Functional Plant Biology, 24 (1997) 407-407.
[47] L.H. Ziska, J.A. Bunce, Influence of increasing carbon dioxide concentration on the photosynthetic and growth stimulation of selected C_4 crops and weeds, Photosynthesis Research, 54 (1997) 199-208.
[48] O. Ghannoum, J.P. Conroy, Nitrogen deficiency precludes a growth response to CO_2 enrichment in C_3 and C_4 *Panicum* grasses, Functional Plant Biology, 25 (1998) 627-636.
[49] D.R. LeCain, J.A. Morgan, Growth, gas exchange, leaf nitrogen and carbohydrate concentrations in NAD-ME and NADP-ME C_4 grasses grown in elevated CO_2, Physiologia Plantarum, 102 (1998) 297-306.
[50] L.H. Ziska, R.C. Sicher, J.A. Bunce, The impact of elevated carbon dioxide on the growth and gas exchange of three C_4 species differing in CO_2 leak rates, Physiologia Plantarum, 105 (1999) 74-80.
[51] S.J.E. Wand, G.F. Midgley, M.H. Jones, P.S. Curtis, Responses of wild C_4 and C_3 grass (Poaceae) species to elevated atmospheric CO_2 concentration: a meta-analytic test of current theories and perceptions, Global Change Biol, 5 (1999) 723-741.

[52] S.J.E. Wand, G.F. Midgley, W.D. Stock, Growth responses to elevated CO_2 in NADP-ME, NAD-ME and PCK C_4 grasses and a C_3 grass from South Africa, Functional Plant Biology, 28 (2001) 13-25.
[53] N. Sionit, D.T. Patterson, Responses of C_4 grasses to atmospheric CO_2 enrichment, Oecol., 65 (1984) 30-34.
[54] J.A. Morgan, H.W. Hunt, C.A. Monz, D.R. Lecain, Consequences of growth at two carbon dioxide concentrations and two temperatures for leaf gas exchange in *Pascopyrum smithii* (C_3) and *Bouteloua gracilis* (C_4), Plant, Cell & Environment, 17 (1994) 1023-1033.
[55] H.H. Rogers, J.F. Thomas, G.E. Bingham, Response of agronomic and forest species to elevated atmospheric carbon dioxide, Science, 220 (1983) 428-429.
[56] M. Stitt, Rising CO_2 levels and their potential significance for carbon flow in photosynthetic cells, Plant, Cell & Environment, 14 (1991) 741-762.
[57] S.C. Wong, Elevated atmospheric partial pressure of CO_2 and plant growth, Oecol., 44 (1979) 68-74.
[58] O. Ghannoum, S.V. Caemmerer, L.H. Ziska, J.P. Conroy, The growth response of C_4 plants to rising atmospheric CO_2 partial pressure: a reassessment, Plant, Cell & Environment, 23 (2000) 931-942.
[59] H. Pinto, R.E. Sharwood, D.T. Tissue, O. Ghannoum, Photosynthesis of C3, C3–C4, and C4 grasses at glacial CO2, Journal of Experimental Botany, 65 (2014) 3669-3681.
[60] S.J.E. Wand, G.F. Midgley, C.F. Musil, Physiological and growth responses of two African species, *Acacia karroo* and *Themeda triandra*, to combined increases in CO_2 and UV‐B radiation, Physiologia Plantarum, 98 (1996) 882-890.
[61] W.J. Bond, G.F. Midgley, F.I. Woodward, M.T. Hoffman, R.M. Cowling, What controls South African vegetation — climate or fire?, South African Journal of Botany, 69 (2003) 79-91.
[62] J.W. Morgan, I.D. Lunt, Effects of time-since-fire on the tussock dynamics of a dominant grass (*Themeda triandra*) in a temperate Australian grassland, Biol. Conserv., 88 (1999) 379-386.
[63] J. Tew, E.S. Grossman, P. Fair, C.F. Cresswell, A study of the fine structure, enzyme activities and pattern of $^{14}CO_2$ incorporation of highveld grasses from different successional stages, Proceedings of the Annual Congresses of the Grassland Society of Southern Africa, 9 (1974) 95-104.
[64] D.G. Ibrahim, M.E. Gilbert, B.S. Ripley, C.P. Osborne, Seasonal differences in photosynthesis between the C_3 and C_4 subspecies of *Alloteropsis semialata* are offset by frost and drought, Plant, Cell & Environment, 31 (2008) 1038-1050.
[65] S.H. Taylor, B.S. Ripley, T. Martin, L.-A. De-Wet, F.I. Woodward, C.P. Osborne, Physiological advantages of C4 grasses in the field: a comparative experiment demonstrating the importance of drought, Global Change Biol, 20 (2014) 1992-2003.
[66] S.H. Taylor, B.S. Ripley, F.I. Woodward, C.P. Osborne, Drought limitation of photosynthesis differs between C_3 and C_4 grass species in a comparative experiment, Plant, Cell & Environment, 34 (2011) 65-75.
[67] C. Bellasio, H. Griffiths, Acclimation to Low Light by C4 maize: Implications for Bundle Sheath Leakiness, Plant Cell Environ, 37 (2014) 1046-1058.
[68] C. Bellasio, M.R. Lundgren, Anatomical constraints to C4 evolution: light harvesting capacity in the bundle sheath, New Phytologist, 212 (2016) 485–496.
[69] C. Bellasio, H. Griffiths, The operation of two decarboxylases (NADPME and PEPCK), transamination and partitioning of C4 metabolic processes between mesophyll and bundle sheath cells allows light capture to be balanced for the maize C4 pathway, Plant Physiol, 164 (2014) 466-480.
[70] C. Bellasio, A generalised stoichiometric model of C3, C2, C2+C4, and C4 photosynthetic metabolism, Journal of Experimental Botany, 68 (2017) 269-282.
[71] A.A. Ali, B.E. Medlyn, T.G. Aubier, K.Y. Crous, P.B. Reich, Elevated carbon dioxide is predicted to promote coexistence among competing species in a trait‐based model, Ecology and Evolution, 5 (2015) 4717-4733.
[72] A.L.S. Swann, F.M. Hoffman, C.D. Koven, J.T. Randerson, Plant responses to increasing CO_2 reduce estimates of climate impacts on drought severity, Proc. Natl. Acad. Sci. U.S.A., 113 (2016) 10019-10024.
[73] S. Zhou, R.A. Duursma, B.E. Medlyn, J.W.G. Kelly, I.C. Prentice, How should we model plant responses to drought? An analysis of stomatal and non-stomatal responses to water stress, Agric. Forest Meteorology, 182-183 (2013) 204-214.

Figures

Figure 1. Schematic representation of the derivation of entities used in the calculation of stomatal (L_S) and non-stomatal (L_{NS}) limitations to assimilation for plants grown at 200 ppm or 800 ppm $[CO_2]_a$. Modelled A-C_i curves showing the response of A_{pot} to C_i for **A** *Vachellia karroo* and **B** C_4 *Eragrostis curvula* grown at either 200 ppm (dashed) or 800 ppm (solid) $_{[CO2]a}$, for illustrative purposes only. Square symbols denote mean A_{op} and C_i (±S.D.) measured under operational conditions. Note how for *E. curvula* (**B**) squares plot at a consistent rate of ~10–11 µmol m^{-2} s^{-1} for plants grown at both 200 ppm (open symbols) and 800 ppm (filled symbols) $[CO_2]_a$, whereas C_{iop} increases with growth $[CO_2]_a$ to become situated beneath the CO_2-saturated part of the A–C_i curve. Leftward-pointing arrows indicate the effect of L_S in the inhibition of A through lowering of C_i relative to C_a. If the decline in C_i is beneath the flatter parts of the A–C_i curve, as it is for plants grown at 800 ppm $[CO_2]_a$, then the reduction in A is minimal (dark grey shading) and L_S is small (Eqn 3). For plants grown at 200 ppm $[CO_2]_a$, the decline in C_i relative to C_a, although smaller than at higher $[CO_2]_a$, occurs beneath the steeper, transitional part of the A–C_i curve and the differential between A_{pot}-C_a and A_{pot}-C_{iop} is larger than at higher growth $[CO_2]_a$. This is reflected in higher L_S. The differential between A_{op} and A_{pot}-C_{iop}, highlighted by the light grey shading, largely determines L_{NS} (Eqn 4).

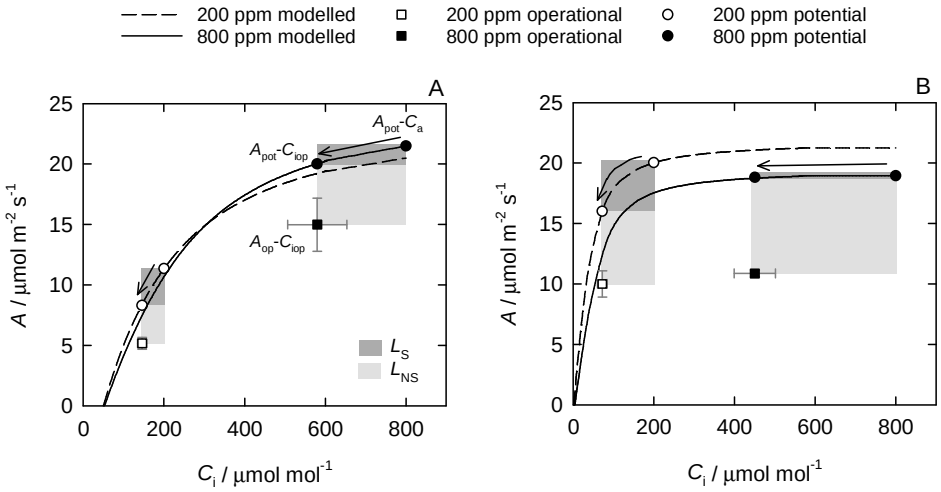

Figure 2. Operational gas exchange measured under growth chamber environmental conditions. Mean ± S.E. operational (**A**) CO_2 assimilation, A_{op} / µmol CO_2 per unit area leaf per second; (**B**) stomatal conductance, g_{Sop} / mol H_2O per unit area leaf per second; (**C**) leaf evapotranspiration, E_{op} / mmol H_2O per unit area leaf per second; (**D**) $[CO_2]$ in the sub-stomatal cavity, C_{iop} / µmol CO_2 per mol air; (**E**) leaf-to-boundary layer water mole fraction gradient, D_S / mmol H_2O per mol air; and (**F**) leaf water potential at midday, Ψ_{leaf} / MPa for three C_3 trees and three C_4 grasses grown at either 200 ppm, 400 ppm or 800 ppm $[CO_2]_a$. Note that symbols have been consistently offset from the true *x*-axis value and connecting lines were introduced for clarity. C_3 trees are *Vachellia karroo* (*n* = 8), *Celtis africana* (*n* = 4-10) and *Combretum apiculatum* (*n* = 4); and C_4 grasses are *Eragrostis curvula* (*n* = 8), *Heteropogon contortus* (*n* = 6) and *Themeda triandra* (*n* = 4). Results of two-way ANOVA testing for effects of species (nested within photosynthetic type), $[CO_2]_a$ and their interaction on each measure are given in Table 2.

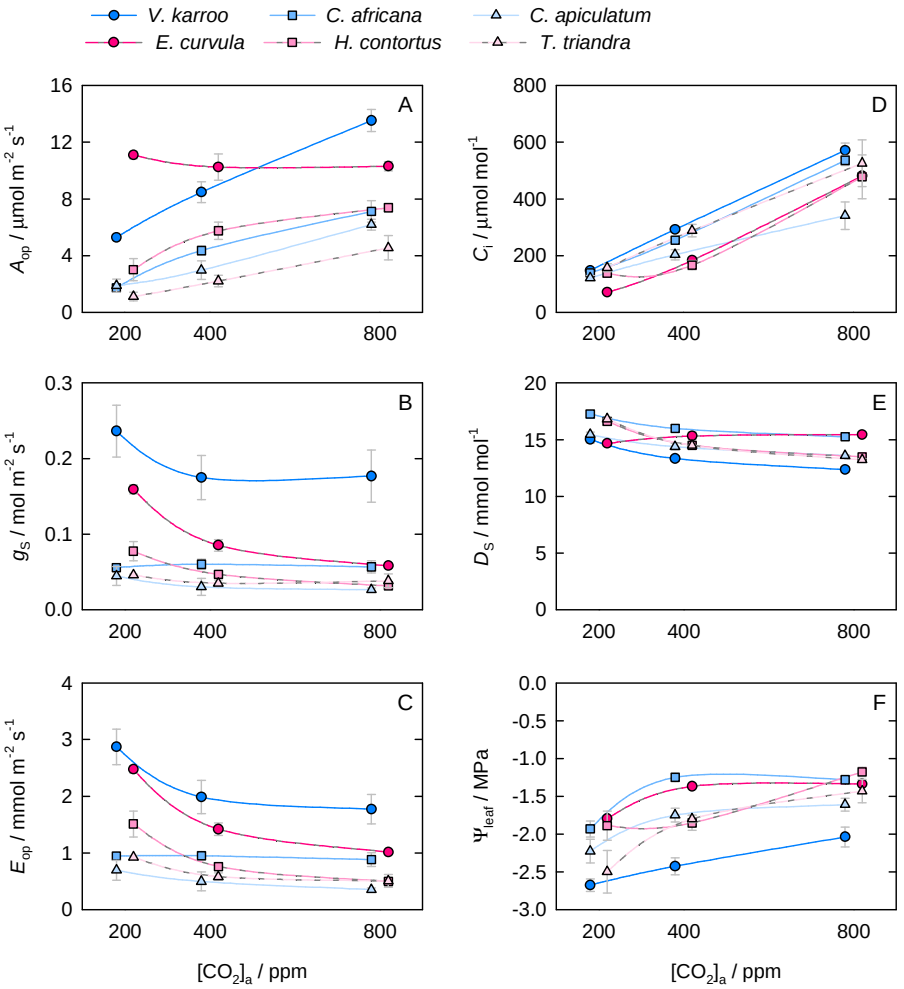

Figure 3. Dependence of assimilation on C_i – observations and simulations from empirical photosynthetic models. Curves show modelled assimilation using empirical models of photosynthesis calculated for each species at variable C_i. C_3 trees (**A**) are *Vachellia karroo* (*n* = 8), *Celtis africana* (*n* = 9-10), and *Combretum apiculatum* (*n* = 4); and C_4 grasses (**B**) are *Eragrostis curvula* (*n* = 8), *Heteropogon contortus* (*n* = 6) and *Themeda triandra* (*n* = 4). Model parameters are listed in Table S1. Symbols show in-cabinet gas exchange measurements under operational growing conditions for C_3 trees (**A**) and C_4 grasses (**B**) grown at 200 ppm (left), 400 ppm (centre), or 800 ppm (right) $[CO_2]_a$.

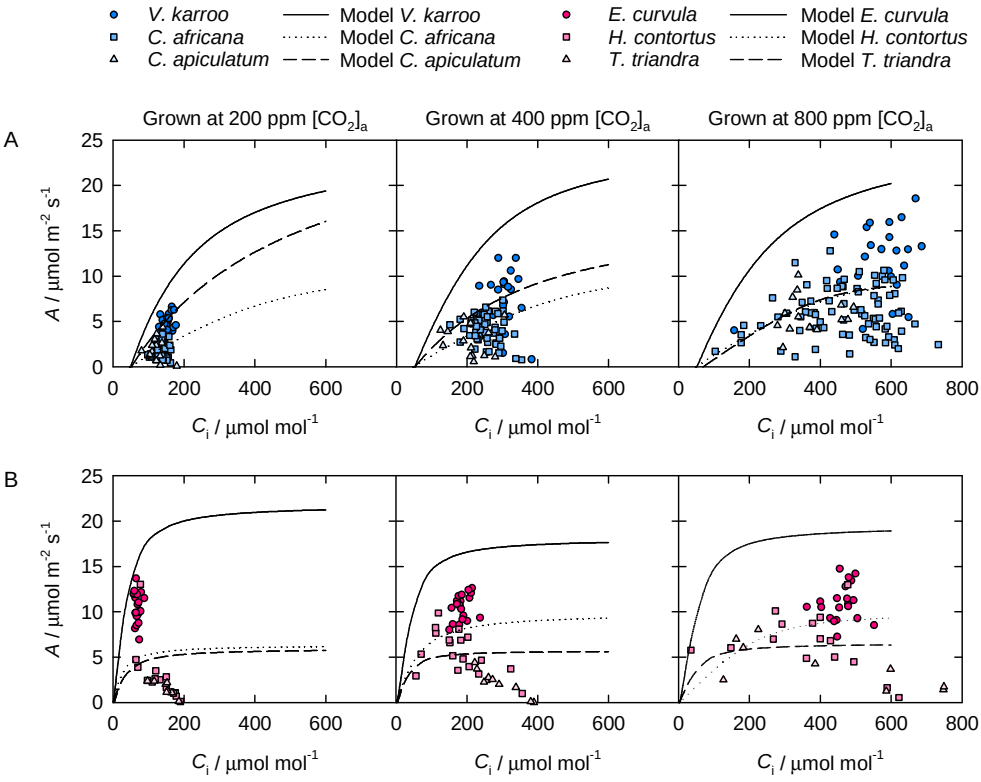

Figure 4. Primary data obtained from gas exchange: *A*–*PPFD* curves. Response of mean ± 1 S.E. photosynthetic CO_2 assimilation (*A*) to increasing photosynthetic photon flux density (*PPFD*) (*A*-*PPFD* curves) measured on leaves of (**A**) C_3 trees *Vachellia karroo*, *Celtis africana* and *Combretum apiculatum* and (**B**) C_4 grasses *Eragrostis curvula*, *Heteropogon contortus* and *Themeda triandra* (grown at 200 ppm (left), 400 ppm (centre), or 800 ppm (right) $[CO_2]_a$ (*n* = 3–6 plants per species×$[CO_2]_a$ treatment).

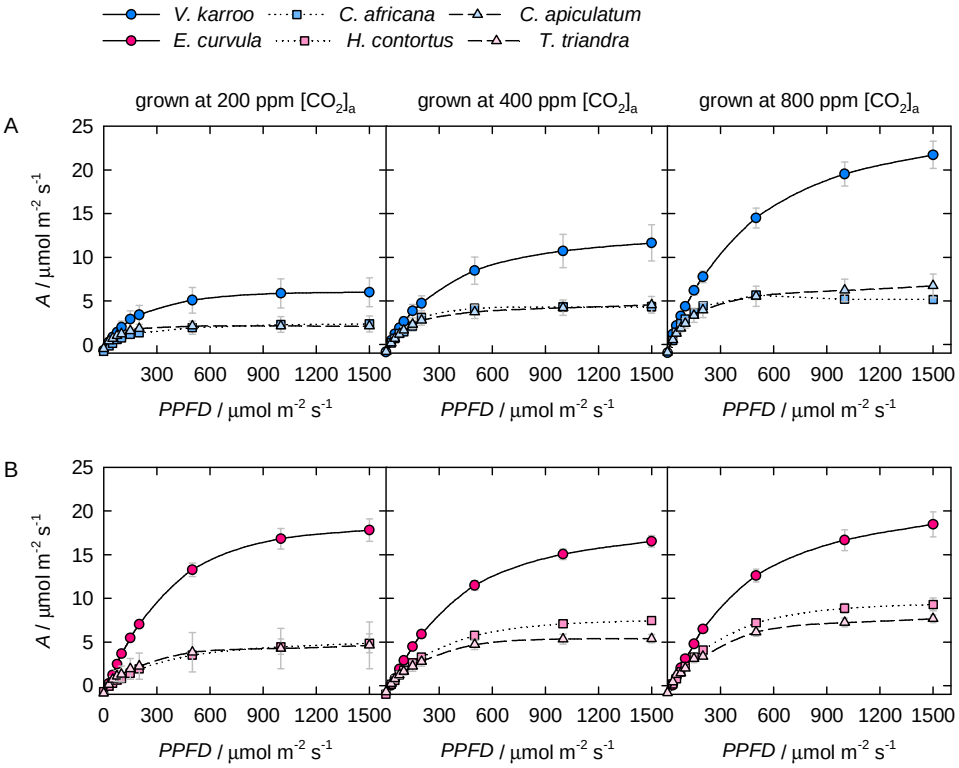

Figure 5. Primary data obtained from gas exchange *A*–C_i curves. Response of mean ± 1 S.E. photosynthetic CO_2 assimilation (*A*) to [CO_2] in the sub-stomatal cavity (C_i) measured on leaves of (**A**) C_3 trees *Vachellia karroo*, *Celtis africana* and *Combretum apiculatum*, and (**B**) C_4 grasses *Eragrostis curvula*, *Heteropogon contortus* and *Themeda triandra* grown at 200 ppm (left), 400 ppm (centre), or 800 (right) ppm $[CO_2]_a$ (*n* = 3–6 plants per species×$[CO_2]_a$ treatment). Horizontal error bars indicate ± 1 S.D. for measured C_i at each C_a setpoint.

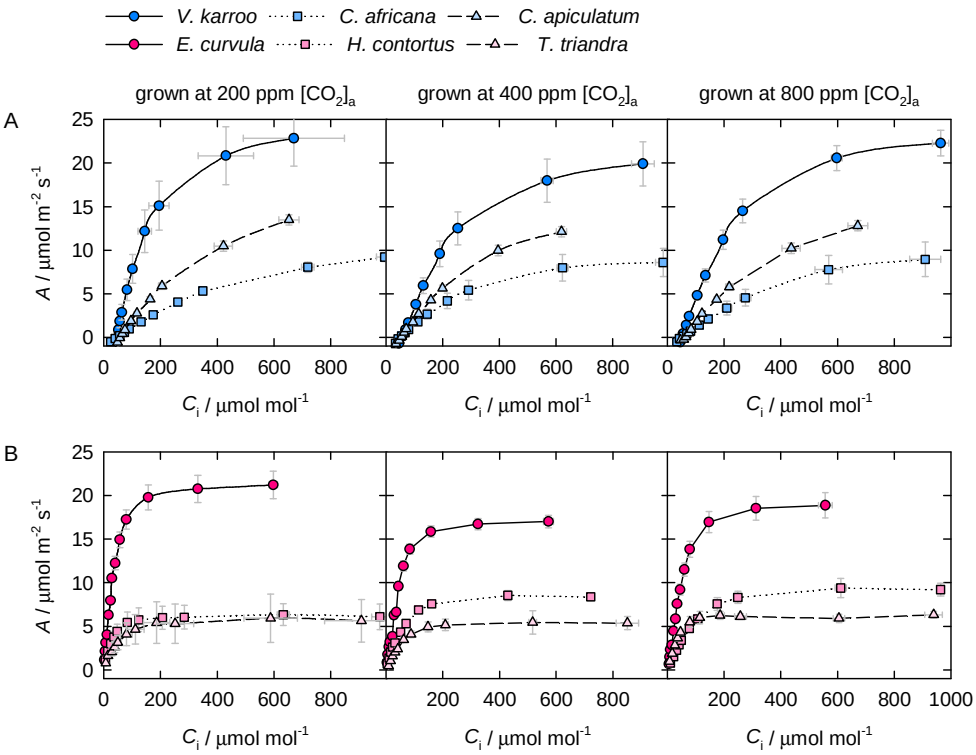

Figure 6. Stomatal and non-stomatal limitations to assimilation. Box plots show stomatal limitation, L_S (**A**–**C**) and non-stomatal limitation, L_{NS} (**D**–**F**) for C_3 trees (blue shades) and C_4 grasses (red shades) grown at either 200 ppm, 400 ppm or 800 ppm $[CO_2]_a$. Boxes show median line with the 25th and 75th percentiles and whiskers show the 10th and 90th percentiles of the data range. C_3 trees are *Vachellia karroo* (*n* = 8), *Celtis africana* (*n* = 9-10), and *Combretum apiculatum* (*n* = 4); and C_4 grasses (**B**) are *Eragrostis curvula* (*n* = 8), *Heteropogon contortus* (*n* = 6) and *Themeda triandra* (*n* = 4). Boxes sharing the same letter range across all treatments are not statistically different at *α* = 0.05, and the dotted lines with grey shading behind groups of boxes denote the mean ± S.E. (*n* = 3) for the C_3 trees and C_4 grasses at each $[CO_2]_a$ level.

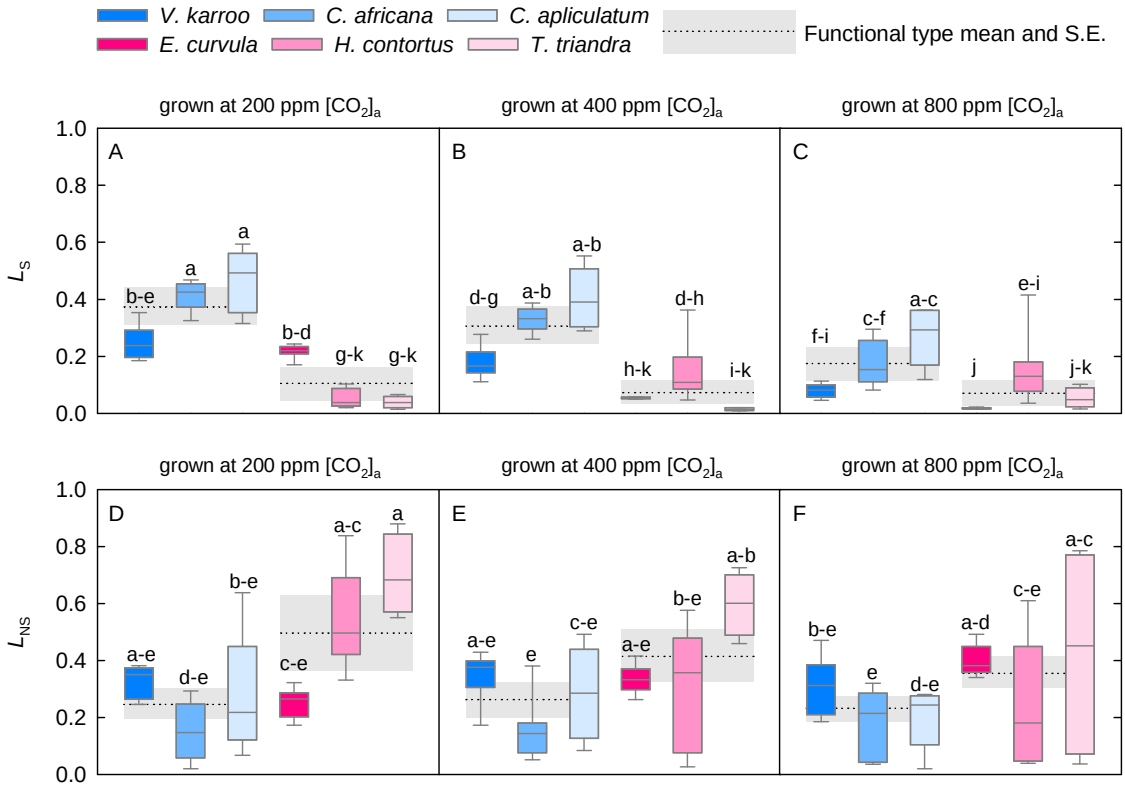

Tables

Table 1. Fitted photosynthetic parameters. Mean values (± 1 S.E.) for parameters derived using *A*–*PPFD* and *A*–C_i response curve fitting within the C_3 and C_4 photosynthesis modelling framework of Bellasio *et al*. (2016a, b) for the three C_3 tree species and three C_4 grass species (n = 3–6 plants per species×$[CO_2]_a$ treatment). ANOVA results for the photosynthetic parameters are listed in Table S2.

			Growth CO_2 concentration			Growth CO_2 concentration			Growth CO_2 concentration		
	Symbol	Units	200 ppm	400 ppm	800 ppm	200 ppm	400 ppm	800 ppm	200 ppm	400 ppm	800 ppm
			Vachellia karroo			*Celtis africana*			*Combretum apiculatum*		
C_3 trees	A_{SAT}	µmol m^{-2} s^{-1}	25.4 (1.11)	24.0 (3.28)	26.7 (1.25)	11.4 (1.41)	11.6 (1.53)	12.5 (1.88)	20.0 (8.56)	19.1 (4.45)	18.9 (1.80)
	CE	mol m^{-2} s^{-1}	0.11 (0.01)	0.09 (0.016)	0.09 (0.012)	0.024 (0.0034)	0.024 (0.0060)	0.025 (0.0050)	0.062 (0.034)	0.047 (0.018)	0.027 (0.0014)
	ω	dimensionless	0.399 (0.105)	0.695 (0.056)	0.622 (0.092)	0.815 (0.166)	0.830 (0.135)	0.899 (0.164)	0.012 (0.012)	0.333 (0.327)	0.930 (0.158)
	Γ	µmol mol^{-1}	49.1 (0.78)	52.6 (2.03)	51.9 (3.65)	45.5 (5.56)	46.6 (3.10)	47.0 (1.34)	50.8 (1.90)	52.5 (0.962)	68.9 (9.76)
	GA_{SAT}	µmol m^{-2} s^{-1}	7.66 (0.47)	17.5 (3.34)	30.2 (3.13)	2.18 (0.302)	6.19 (1.10)	9.37 (1.33)	3.68 (0.721)	6.48 (2.40)	9.33 (0.272)
	$Y(CO_2)_{LL}$	dimensionless	0.030 (0.005)	0.050 (0.008)	0.060 (0.004)	0.027 (0.0042)	0.036 (0.0060)	0.043 (0.0078)	0.025 (0.0078)	0.043 (0.022)	0.074 (0.016)
	m	dimensionless	0.272 (0.180)	0.113 (0.069)	0.524 (0.122)	0.336 (0.178)	0.501 (0.117)	0.441 (0.025)	0.352 (0.354)	0.569 (0.269)	0.388 (0.099)
	LCP	µmol m^{-2} s^{-1}	15.7 (3.54)	13.1 (2.78)	12.1 (2.14)	30.1 (17.2)	24.3 (5.13)	17.2 (2.41)	42.5 (15.3)	32.8 (7.28)	28.5 (8.13)
	R_{LIGHT}	>0 µmol m^{-2} s^{-1}	0.43 (0.005)	0.53 (0.122)	0.72 (0.139)	0.396 (0.054)	0.747 (0.153)	0.653 (0.138)	0.786 (0.035)	1.12 (0.298)	1.49 (0.0050)
			Eragrostis curvula			*Heteropogon contortus*			*Themeda triandra*		
C_4 grasses	A_{SAT}	µmol m^{-2} s^{-1}	21.8 (1.59)	17.5 (0.748)	19.5 (1.42)	6.36 (1.63)	9.91 (1.96)	10.1 (1.97)	6.01 (3.25)	5.69 (0.953)	6.63 (0.184)
	CE	dimensionless	0.38 (0.039)	0.29 (0.026)	0.25 (0.018)	0.193 (0.0064)	0.125 (0.0027)	0.040 (0.0085)	0.123 (0.021)	0.106 (0.018)	0.091 (0.019)
	ω	dimensionless	0.751 (0.047)	0.777 (0.037)	0.804 (0.033)	0.485 (0.312)	0.589 (0.025)	0.878 (0.0085)	0.569 (0.216)	0.799 (0.075)	0.777 (0.115)
	Γ	µmol mol^{-1}	1.49 (0.580)	3.85 (1.18)	3.99 (0.980)	0.0 (0.0)	0.0 (0.0)	2.74 (0.545)	5.95 (0.940)	5.74 (1.85)	6.57 (0.693)
	GA_{SAT}	µmol m^{-2} s^{-1}	20.4 (1.79)	20.1 (1.10)	21.6 (1.66)	6.91 (2.35)	9.92 (0.092)	12.04 (1.16)	5.99 (3.79)	7.16 (0.337)	9.97 (0.416)
	$Y(CO_2)_{LL}$	dimensionless	0.050 (0.0035)	0.050 (7.6×10^{-4})	0.050 (0.0035)	0.021 (0.0014)	0.038 (0.0013)	0.021 (0.0014)	0.035 (0.017)	0.036 (0.0075)	0.041 (0.0058)
	m	dimensionless	0.421 (0.088)	0.158 (0.053)	0.395 (0.053)	0.075 (0.078)	0.369 (0.179)	0.0 (0.071)	0.0 (0.0)	0.0 (0.0)	0.074 (0.076)
	LCP	µmol m^{-2} s^{-1}	25.1 (2.09)	30.1 (1.49)	30.5 (2.210)	34.5 (12.6)	26.9 (0.155)	49.3 (6.61)	35.9 (16.9)	24.1 (8.37)	19.5 (1.00)
	R_{LIGHT}	>0 µmol m^{-2} s^{-1}	1.25 (0.092)	1.37 (0.083)	1.38 (0.113)	0.644 (0.195)	0.938 (0.030)	0.847 (0.095)	0.786 (0.120)	0.700 (0.099)	0.701 (0.061)

A*$_{SAT}$**, CO_2-saturated assimilation measured in *A*–C_i curve; ***CE, carboxylating efficiency, initial slope of the *A*–C_i curve; **Γ**, C_i–*A* compensation point, i.e. C_i where *A* = 0; ***GA*$_{SAT}$**, Light-saturated gross assimilation at $[CO_2]_a$ of light curve; ***LCP***, PPFD–*A* compensation point, i.e. *PPFD* where *A* = 0; ***R*$_{LIGHT}$**, Respiration in the light/day; ***Y(CO$_2$)$_{LL}$***, initial (or maximum) quantum yield for CO_2 fixation.

Table 2. Output from ANOVA tests on operational gas exchange and leaf water potential. Results of two-way ANOVAs testing for effects of species nested within photosynthesis type [C_3 trees: *Vachellia karroo* (*n* = 8), *Celtis africana* (*n* = 4-10), and *Combretum apiculatum* (*n* = 4); and C_4 grasses: *Eragrostis curvula* (*n* = 8), *Heteropogon contortus* (*n* = 6), and *Themeda triandra* (*n* = 4)], $[CO_2]_a$, (200 ppm, 400 ppm, or 800 ppm) and the interaction of species and $[CO_2]_a$. Mean values ± S.E. are plotted in Figure 2. Assumptions of homogeneity of variance for the model were satisfied by transforming datasets as indicated.

		Species (nested within photosynthesis type, PT)			**$[CO_2]_a$**			**Spp.(nested in PT) × $[CO_2]_a$**		
Symbol	**Units**	**d.f.**	***F***	***P***	**d.f.**	***F***	***P***	**d.f.**	***F***	***P***
A_{op} [a]	µmol m^{-2} s^{-1}	**4, 110**	**67.2**	**<0.0001**	**2, 110**	**69.6**	**<0.0001**	**8, 110**	**4.59**	**<0.0001**
g_{Sop} [a]	mol m^{-2} s^{-1}	**4, 110**	**59.6**	**<0.0001**	**2, 110**	**13.8**	**<0.0001**	8, 110	1.18	0.320
E_{op} [a]	mmol m^{-2} s^{-1}	**4, 110**	**56.5**	**<0.0001**	**2, 110**	**27.2**	**<0.0001**	8, 110	1.11	0.361
D_S	µmol mol^{-1}	**4, 110**	**58.7**	**<0.0001**	**2, 110**	**100.8**	**<0.0001**	**8, 110**	**13.2**	**<0.0001**
C_i [b]	µmol mol^{-1}	**4, 110**	**5.18**	**0.001**	**2, 110**	**51.9**	**<0.0001**	**8, 110**	**12.8**	**<0.0001**
Ψ_{leaf} [a]	MPa	**4, 110**	**10.5**	**<0.0001**	**2, 110**	**11.4**	**<0.0001**	**8, 110**	**2.65**	**0.011**

[a] Data subjected to Johnson Transformation to achieve normality of variance:
A_{op}: 0.6402+0.9252·Ln((*x*+0.1988)/18.512−*x*)
g_S: -1.5724+1.0060·Asinh((*x*-0.02414)/0.01677)
E_{op}: -0.1204+1.6636·Ln(*x*+0.03846)
Ψ_{leaf}: 0.9394+1.0060·Ln((*x*-0.9234)/(3.5548-*x*)
[b] natural log. transformed

Table 3. Output from ANOVA tests on fitted parameters of the photosynthesis models and stomatal and non-stomatal limitations to photosynthesis. Results of two-way ANOVAs testing for effects of species nested within photosynthesis type [C_3 trees: *Vachellia karroo*, *Celtis africana*, and *Combretum apiculatum*; and C_4 grasses: *Eragrostis curvula*, *Heteropogon contortus*, and *Themeda triandra*], $[CO_2]_a$, (200 ppm, 400 ppm, or 800 ppm) and the interaction of species and $[CO_2]_a$ on photosynthetic parameters. Assumptions of homogeneity of variance for the model were satisfied by transforming datasets as indicated.

		Species (nested within photosynthesis type, PT)			**$[CO_2]_a$**			**Spp.(nested in PT) × $[CO_2]_a$**		
Symbol	**Units**	**d.f.**	***F***	***P***	**d.f.**	***F***	***P***	**d.f.**	***F***	***P***
A_{SAT} [a]	µmol m^{-2} s^{-1}	**4, 71**	**21.6**	**<0.0001**	2, 71	0.32	0.725	8, 71	2.74	0.084
CE [b]	mol m^{-2} s^{-1}	**4, 71**	**23.3**	**<0.0001**	**2, 71**	**3.14**	**0.049**	**8, 71**	**4.55**	**<0.0001**
Γ [c]	µmol mol^{-1}	4, 71	1.43	0.271	**2, 71**	**8.08**	**0.001**	8, 71	1.27	0.271
ω [c]	dimensionless	4, 71	1.62	0.178	**2, 71**	**3.28**	**0.043**	8, 71	0.80	0.605
GA_{SAT} [a]	µmol m^{-2} s^{-1}	**4, 71**	**34.7**	**<0.0001**	**2, 71**	**10.73**	**<0.0001**	**8, 71**	**4.16**	**<0.0001**
LCP [b]	µmol m^{-2} s^{-1}	**4, 71**	**4.12**	**0.005**	2, 71	0.03	0.971	8, 71	0.69	0.701
R_{LIGHT} [b]	>0 µmol m^{-2} s^{-1}	**4, 71**	**6.93**	**<0.0001**	**2, 71**	**5.97**	**0.004**	8, 71	0.98	0.459
m	dimensionless	**4, 71**	**4.13**	**0.004**	2, 71	2.12	0.127	8, 71	1.43	0.197
$Y(CO_2)_{LL}$	dimensionless	**4, 71**	**5.19**	**0.001**	**2, 71**	**8.06**	**0.001**	**8, 71**	**1.35**	**0.006**
L_S [c]	dimensionless	**4, 110**	**25.3**	**<0.0001**	**2, 110**	**31.7**	**<0.0001**	**8, 110**	**7.81**	**<0.0001**
L_{NS} [c]	dimensionless	**4, 110**	**14.5**	**<0.0001**	2, 110	1.15	0.319	**8, 110**	**3.07**	**0.004**

Data transformations: [a]√; [b]natural log.; [c]arcsine(√).